Scientia Iranica B (2019) 26(6), 3356–3368

SCIENTIA IRANICA

Sharif University of Technology
Scientia Iranica
Transactions B: Mechanical Engineering
http://scientiairanica.sharif.edu

Research Note

A collocation algorithm based on quintic B-splines for the solitary wave simulation of the GRLW equation

H. Zeybek[a,*] and S. Battal Gazi Karakoç[b]

a. *Department of Applied Mathematics, Faculty of Computer Science, Abdullah Gül University, 38080 Kayseri, Turkey.*
b. *Department of Mathematics, Faculty of Science and Art, Nevşehir Hacı Bektaş Veli University, 50300, Nevşehir, Turkey.*

Received 22 January 2017; received in revised form 21 January 2018; accepted 21 July 2018

KEYWORDS
GRLW equation;
Finite element scheme;
Quintic B-spline;
Solitons;
Undular bore.

Abstract. In this article, a collocation algorithm based on quintic B-splines is proposed to find a numerical solution to the nonlinear Generalized Regularized Long Wave (GRLW) equation. Moreover, to analyze the linear stability of the numerical scheme, the von-Neumann technique is used. The numerical approach to three test examples consisting of a single solitary wave, the collision of two solitary waves, and the growth of an undular bore is discussed. The accuracy of the method is demonstrated by calculating the error in L_2 and L_∞ norms and the conservative quantities I_1, I_2 and I_3. The findings are compared with those previously reported in the literature. Finally, the motion of solitary waves is graphically plotted according to different parameters.

1. Introduction

The nonlinear wave phenomenon has an instrumental role in predicting natural events. The long waves in water of varying depths are modeled by equations of motion. The equations introduced for small amplitude waves are of nonlinear terms. The Regularized Long Wave (RLW) equation was initially introduced as a model for small-amplitude long waves on the surface of water in a channel by Peregrine [1,2]. Here, Peregrine examined the growth of an undular bore from a long wave. According to him, when the long wave of elevation travels in shallow water, it steepens and forms a bore. The RLW equation was discussed as an improved model of more common Korteweg-de Vries (KdV) equation by Benjamin et al. [3]. The KdV equation defines long waves by assuming a small wave amplitude and a large wave length in nonlinear dispersive and many other physical systems. Then, the idea of Equal Width (EW) wave equation, which has both positive and negative amplitudes with the same width, was proposed by Morrison et al. [4]. Therefore, the Generalized Regularized Long Wave (GRLW) equation and the Generalized Equal Width (GEW) wave equation offer some technical advantages over the Generalized Korteweg-de Vries (GKdV) equation. Such types of wave equations have solitary wave solutions, which are pulse-like.

The nonlinear GKdV equation has the following form:

$$U_t + \varepsilon U^p U_x + \mu U_{xxx} = 0. \tag{1}$$

The nonlinear GEW equation is described as follows:

$$U_t + \varepsilon U^p U_x - \mu U_{xxt} = 0, \tag{2}$$

and the nonlinear GRLW equation, discussed here, is given by:

$$U_t + U_x + p(p+1)U^p U_x - \mu U_{xxt} = 0, \tag{3}$$

subject to physical boundary conditions $U \to 0$ as

*. *Corresponding author.*
E-mail addresses: zeybek.halil45@gmail.com (H. Zeybek); sbgkarakoc@nevsehir.edu.tr (S. Battal Gazi Karakoç)

doi: 10.24200/sci.2018.20781

$x \to \pm\infty$, in which subscripts t and x represent time and spatial differentiations, ε and p are the positive integers, and μ is the positive constant. The boundary and initial conditions are assumed to be as follows:

$$U(a,t)=0, \qquad U(b,t)=0, \qquad t>0,$$

$$U_x(a,t)=0, \qquad U_x(b,t)=0, \qquad t>0,$$

$$U(x,0)=f(x), \qquad a\le x\le b, \tag{4}$$

where $f(x)$ is the prescribed function at the interval $[a,b]$ and will be determined next. In the fluid problems, U is related to the vertical displacement of the water surface or a similar physical quantity. In the plasma applications, U defines the negative of the electrostatic potential. Hence, the solitary wave solution of Eqs. (1) to (3) reveals what many physical phenomena with weak nonlinearity and dispersion waves such as nonlinear transverse waves in shallow water, ion-acoustic, and magnetohydrodynamic waves in plasma and phonon packets in nonlinear crystals mean.

Indeed, the nonlinear RLW equation is formed by obtaining $p = 1$ in Eq. (3). In the literature, there are large quantities of studies on the RLW equation. In the 1960s, Peregrine studied the RLW equation with the growth of an undular bore [1,2]. The approximate analytical method for the simulation of wave propagation in the nonlinear RLW equation was investigated by Morrison et al. [4]. Quadratic B-spline collocation algorithm for the nonlinear RLW equation was proposed by Raslan [5]. The RLW equation was solved numerically by using collocation algorithm based on cubic, septic, quantic, and sextic B-splines [6-9]. Galerkin finite-element method with quintic, quadratic B-splines was used to find numerical solutions of the one-dimensional RLW equation by Dağ et al. [10] and Esen and Kutluay [11]. The new Galerkin method was set up by Mei and Chen by using linear finite elements for the RLW equation [12].

In the case of $p = 2$, Eq. (3) is known as the Modified Regularized Long Wave (MRLW) equation. The numerical solution to the MRLW equation was found by using a collocation method based on quintic, cubic, quartic, and septic B-splines [13-18]. Ali employed the method of mesh free to obtain a numerical solution to the MRLW equation [19]. Collocation algorithm has been newly set up with extended cubic B-splines for the numerical calculation of the MRLW equation by Dag et al. [20]. Moreover, the multi-grid method was developed for the numerical calculation of the MRLW equation by Abo Essa et al. [21].

So far, solitary wave solutions of the nonlinear GRLW equation have been found with some solution techniques by many researchers. Bona et al. [22] obtained both stable and unstable solitary-wave solutions of the nonlinear GRLW equation. Numerical methods based on finite difference scheme, He's variational iteration scheme, mesh-free technique, Petrov-Galerkin scheme, element-free approximation, and second-order compact finite difference scheme were introduced for GRLW equation [23-28]. The generalized KdV and RLW equations were solved exactly and numerically by using Adomian decomposition method [29]. Hamdi et al. [30] investigated the new exact solution approach to GRLW and its simpler alternative model, GEW equation. An approximate quasilinearization technique was designed to obtain the solitary wave solutions to nonlinear GRLW equation with an initial condition on the effects of undular bore by Ramos [31]. Mohammadi [32] obtained a numerical solution to the nonlinear GRLW equation using collocation algorithm based on exponential B-spline finite elements. Zeybek and Karakoç used a finite element method with B-splines to solve the GRLW equation [33,34]. Lately, collocation scheme based on B-spline finite elements was investigated for solving the Complex Modified Korteweg-de Vries (CMKdV), the generalized nonlinear Schrodinger (GNLS) equation, and generalized Burgers-Fisher and Burgers-Huxley equations [35-37]. Moreover, Petrov-Galerkin finite element method based on B-splines was presented for the numerical calculation of the modified Korteweg-de Vries (mKdV) equation by Ak et al. [38].

Considering the numerical algorithms applied to a similar type of nonlinear equations; in this paper, we have implemented the quintic B-spline collocation approach to GRLW equation.

2. Numerical algorithm: Quintic B-spline collocation method

Consider a partition of the interval $[a,b]$ into N equal subintervals by the points x_m, $m=0,1,\cdots N$ such that $h=\frac{b-a}{N}=(x_{m+1}-x_m)$. The set of quintic B-spline functions $\{\phi_{-2}(x),\phi_{-1}(x),\cdots,\phi_{N+2}(x)\}$ at the knots x_m forming a basis for the functions defined over the solution region $[a,b]$ is introduced by Prenter [39] (see Eq. (5) in Box I). Each quintic B-spline, ϕ_m, covers 6 elements; therefore, each finite element $[x_m,x_{m+1}]$ is covered by 6 splines. The numerical approximation, $U_N(x,t)$, is described with the quintic B-spline functions by:

$$U_N(x,t)=\sum_{m=-2}^{N+2}\phi_m(x)\delta_m(t), \tag{6}$$

where $\delta_m(t)$ is the unknown time-dependent parameter and is calculated within the boundary conditions and collocation forms. By substituting B-spline functions (5) into approximate function (6), the nodal values of U_m, U'_m, U''_m with regard to δ_m are derived as follows:

$$\phi_m(x)=\frac{1}{h^5}\begin{cases}(x-x_{m-3})^5, & [x_{m-3},x_{m-2})\\ (x-x_{m-3})^5-6(x-x_{m-2})^5, & [x_{m-2},x_{m-1})\\ (x-x_{m-3})^5-6(x-x_{m-2})^5+15(x-x_{m-1})^5, & [x_{m-1},x_m)\\ (x_{m+3}-x)^5-6(x_{m+2}-x)^5+15(x_{m+1}-x)^5, & [x_m,x_{m+1})\\ (x_{m+3}-x)^5-6(x_{m+2}-x)^5, & [x_{m+1},x_{m+2})\\ (x_{m+3}-x)^5, & [x_{m+2},x_{m+3}]\\ 0, & \text{otherwise}\end{cases} \quad (5)$$

Box I

$$U_N(x_m,t)=U_m=\delta_{m-2}+26\delta_{m-1}+66\delta_m+26\delta_{m+1}+\delta_{m+2},$$

$$U'_m=\frac{5}{h}(-\delta_{m-2}-10\delta_{m-1}+10\delta_{m+1}+\delta_{m+2}),$$

$$U''_m=\frac{20}{h^2}(\delta_{m-2}+2\delta_{m-1}-6\delta_m+2\delta_{m+1}+\delta_{m+2}), \quad (7)$$

and the variation of U over the element $[x_m,x_{m+1}]$ is written by:

$$U=\sum_{m=-2}^{N+2}\phi_m\delta_m. \quad (8)$$

Using the nodal values of U_m and their space derivatives given by Eq. (7) in Eq. (3), we get:

$$\left(\dot{\delta}_{m-2}+26\dot{\delta}_{m-1}+66\dot{\delta}_m+26\dot{\delta}_{m+1}+\dot{\delta}_{m+2}\right)+\frac{5}{h}(-\delta_{m-2}-10\delta_{m-1}+10\delta_{m+1}+\delta_{m+2})+p(p+1)Z_m(\delta_{m-2}+26\delta_{m-1}+66\delta_m+26\delta_{m+1}+\delta_{m+2})-\frac{20\mu}{h^2}\left(\dot{\delta}_{m-2}+2\dot{\delta}_{m-1}-6\dot{\delta}_m+2\dot{\delta}_{m+1}+\dot{\delta}_{m+2}\right)=0, \quad (9)$$

where '$\cdot$' represents the derivative of time and:

$$Z_m=(U_m)^{p-1}(U_m)_x.$$

If the Rubin and Graves' linearization approach [40] is applied to $U^{p-1}U_x$, we have the following formula:

$$\left(U^{p-1}U_x\right)^{n+1}=\left(U^{p-1}\right)^n(U_x)^{n+1}+\left(U^{p-1}\right)^{n+1}(U_x)^n-\left(U^{p-1}\right)^n(U_x)^n. \quad (10)$$

The implementation of the Crank-Nicolson formula, $\delta_m=\frac{1}{2}(\delta_m^n+\delta_m^{n+1})$, and usual forward difference approach, $\dot{\delta}_m=\frac{\delta_m^{n+1}-\delta_m^n}{\Delta t}$, to Eq. (9) leads to the following recurrence relation:

$$\gamma_1\delta_{m-2}^{n+1}+\gamma_2\delta_{m-1}^{n+1}+\gamma_3\delta_m^{n+1}+\gamma_4\delta_{m+1}^{n+1}+\gamma_5\delta_{m+2}^{n+1}=\gamma_6\delta_{m-2}^n+\gamma_7\delta_{m-1}^n+\gamma_8\delta_m^n+\gamma_9\delta_{m+1}^n+\gamma_{10}\delta_{m+2}^n, \quad (11)$$

where:

$$\gamma_1=(1-K+EZ_m-M),$$

$$\gamma_2=(26-10K+26EZ_m-2M),$$

$$\gamma_3=(66+66EZ_m+6M),$$

$$\gamma_4=(26+10K+26EZ_m-2M),$$

$$\gamma_5=(1+K+EZ_m-M),$$

$$\gamma_6=(1+K-EZ_m-M),$$

$$\gamma_7=(26+10K-26EZ_m-2M),$$

$$\gamma_8=(66-66EZ_m+6M),$$

$$\gamma_9=(26-10K-26EZ_m-2M),$$

$$\gamma_{10}=(1-K-EZ_m-M),$$

$$m=0,1,\cdots,N, \qquad K=\frac{5\Delta t}{2h},$$

$$E=\frac{p(p+1)\Delta t}{2}, \qquad M=\frac{20\mu}{h^2}. \quad (12)$$

The recurrence relation (11) comprises $(N+1)$ linear equations, whereas this system involves $(N+5)$ unknowns $(\delta_{-2},\delta_{-1},\cdots,\delta_{N+1},\delta_{N+2})^T$. Using the boundary conditions given by Eq. (4), we delete δ_{-2},δ_{-1} and $\delta_{N+1},\delta_{N+2}$ from Systems (11). In this case, the penta-diagonal matrix system can be easily achieved as follows:

$$A\mathbf{d}^{\mathbf{n+1}}=B\mathbf{d}^{\mathbf{n}}, \quad (13)$$

which can be solved through the penta-diagonal system. To obtain better numerical results at each time step, two or three inner iterations $\delta^{n*}=\delta^n+\frac{1}{2}(\delta^n-\delta^{n-1})$ are applied to Z_m.

In order to start the iteration, initial parameters d^0 must be computed by using the following conditions:

$$U_N(x,0)=U(x_m,0), \qquad m=0,1,2,\cdots,N,$$

$$(U_N)_x(a,0)=0, \qquad (U_N)_x(b,0)=0,$$

$$(U_N)_{xx}(a,0)=0, \qquad (U_N)_{xx}(b,0)=0.$$

Therefore, we have the ratio of the matrix equation to the initial vector d^0:

$$Wd^0=b,$$

where:

$$W=\begin{bmatrix} 54 & 60 & 6 & & & & & \\ 25.25 & 67.5 & 26.25 & 1 & & & & \\ 1 & 26 & 66 & 26 & 1 & & & \\ & & \ddots & \ddots & \ddots & \ddots & & \\ & & & 1 & 26 & 66 & 26 & 1 \\ & & & & 1 & 26.25 & 67.5 & 25.25 \\ & & & & & 6 & 60 & 54 \end{bmatrix},$$

$$d^0=(\delta_0,\delta_1,\delta_2,\cdots,\delta_{N-2},\delta_{N-1},\delta_N)^T,$$

$$b=(U(x_0,0),U(x_1,0),\cdots,U(x_{N-1},0),U(x_N,0))^T.$$

2.1. The solution with penta-diagonal algorithm

Designed in the Fortran program, the solution method with penta-diagonal algorithm is given as follows: The penta-diagonal system can be written as follows:

$$a_i\delta_{i-2}+b_i\delta_{i-1}+c_i\delta_i+d_i\delta_{i+1}+e_i\delta_{i+2}=f_i,$$

$$i=0,1,\cdots,N.$$

Firstly, the parameters are established with:

$$\alpha_0=0, \qquad \beta_0=c_0, \qquad \mu_0=\frac{d_0}{\beta_0}, \qquad \zeta_0=\frac{e_0}{\beta_0},$$

$$\lambda_0=\frac{f_0}{\beta_0}, \qquad \alpha_1=b_0, \qquad \beta_1=c_1-\alpha_1\mu_0,$$

$$\mu_1=\frac{d_1-\alpha_1\zeta_0}{\beta_1}, \qquad \zeta_1=\frac{e_1}{\beta_1}, \qquad \lambda_1=\frac{f_1-\alpha_1\lambda_0}{\beta_1}.$$

Afterwards, the following parameters are computed:

$$\alpha_i=b_{i-1}-a_{i-2}\mu_{i-2}, \qquad \beta_i=c_i-\alpha_i\mu_{i-1}-a_{i-2}\zeta_{i-2},$$

$$\mu_i=\frac{d_i-\alpha_i\zeta_{i-1}}{\beta_i}, \qquad \zeta_i=\frac{e_i}{\beta_i},$$

$$\lambda_i=\frac{f_i-\alpha_i\lambda_{i-1}-a_{i-2}\lambda_{i-2}}{\beta_i},$$

$$\text{for} \quad i=2,3,\cdots,N.$$

Now, the solution is obtained as follows:

$$\delta_i=\lambda_i-\zeta_i\delta_{i+2}-\mu_i\delta_{i+1},$$

$$i=0,1,\cdots,N-3,N-2,$$

$$\delta_{N-1}=\lambda_{N-1}-\mu_{N-1}\delta_N, \qquad \delta_N=\lambda_N.$$

2.2. Stability of the scheme

To ensure the stability of the scheme, the von-Neumann technique is followed. Moreover, U^p in the nonlinear term is considered to be locally constant. If the same steps in the presented numerical algorithm are performed, the following recurrence relation is obtained:

$$\alpha_1\delta_{m-2}^{n+1}+\alpha_2\delta_{m-1}^{n+1}+\alpha_3\delta_m^{n+1}+\alpha_4\delta_{m+1}^{n+1}+\alpha_5\delta_{m+2}^{n+1}$$
$$=\alpha_5\delta_{m-2}^{n}+\alpha_4\delta_{m-1}^{n}+\alpha_3\delta_m^{n}+\alpha_2\delta_{m+1}^{n}+\alpha_1\delta_{m+2}^{n}, \tag{14}$$

where:

$$\alpha_1=(1-K-KEZ_m-M),$$

$$\alpha_2=(26-10K-10KEZ_m-2M),$$

$$\alpha_3=(66+6M),$$

$$\alpha_4=(26+10K+10KEZ_m-2M),$$

$$\alpha_5=(1+K+KEZ_m-M), \qquad m=0,1,\cdots,N,$$

$$K=\frac{5\Delta t}{2h}, \qquad E=\frac{p(p+1)\Delta t}{2}, \qquad M=\frac{20\mu}{h^2}. \tag{15}$$

Then, the Fourier mode $\delta_m^n=\xi^n e^{imkh}$, where $i=\sqrt{-1}$, h is the step length, and k is the mode number in the above equation, which produces the following equality:

$$\alpha_1\xi^{n+1}e^{i(m-2)kh}+\alpha_2\xi^{n+1}e^{i(m-1)kh}+\alpha_3\xi^{n+1}e^{imkh}$$
$$+\alpha_4\xi^{n+1}e^{i(m+1)kh}+\alpha_5\xi^{n+1}e^{i(m+2)kh}$$
$$=\alpha_5\xi^{n}e^{i(m-2)kh}+\alpha_4\xi^{n}e^{i(m-1)kh}+\alpha_3\xi^{n}e^{imkh}$$
$$+\alpha_2\xi^{n}e^{i(m+1)kh}+\alpha_1\xi^{n}e^{i(m+2)kh}. \tag{16}$$

Implementing Euler's formula ($e^{ikh}=\cos(kh)+i\sin(kh)$), we get:

$$\xi=\frac{a-ib}{a+ib},$$

in which:

$$a=\alpha_3+(\alpha_4+\alpha_2)\cos[hk]+(\alpha_5+\alpha_1)\cos[2hk],$$

$$b=(\alpha_4-\alpha_2)\sin[hk]+(\alpha_5-\alpha_1)\sin[2hk].$$

The modulus of $|\xi|$ is 1, making the linearized scheme unconditionally stable.

3. Numerical examples and results

In this part, the numerical approach is implemented on three examples containing a single solitary wave, the collision of two solitary waves, and the growth of an undular bore. The error in L_2 and L_∞ norms is computed to check the efficiency and accuracy of the numerical scheme. To this end, the exact solution of GRLW equation given in Eq. (17) and the following formulas are used:

$$L_2 = \left\| U^{\text{exact}} - U_N \right\|_2 \simeq \sqrt{h \sum_{J=0}^{N} \left| U_j^{\text{exact}} - (U_N)_j \right|^2},$$

$$L_\infty = \left\| U^{\text{exact}} - U_N \right\|_\infty \simeq \max_j \left| U_j^{\text{exact}} - (U_N)_j \right|.$$

The papers [13,25] presented the exact solution to GRLW equation as follows:

$$U(x,t) = \sqrt[p]{\frac{v(p+2)}{2p}} \sec h^2 \left[\frac{p}{2} \sqrt{\frac{v}{\mu(v+1)}} (x-(v+1)t-x_0) \right], \tag{17}$$

where $v+1$ is the velocity of the wave in the direction of propagation, x_0 is the arbitrary constant, and $\sqrt[p]{\frac{v(p+2)}{2p}}$ defines amplitude. In addition, to register that the numerical scheme retains the physical quantities, the changes of the invariants related to mass, momentum, and energy are studied.

$$I_1 = \int_a^b U dx, \qquad I_2 = \int_a^b \left[U^2 + \mu (U_x)^2 \right] dx,$$

$$I_3 = \int_a^b \left[U^4 - \mu (U_x)^2 \right] dx. \tag{18}$$

3.1. Example 1: A single solitary wave

The first test example is established with the initial condition of $t = 0$ in Eq. (17). In order to achieve uniform and comparable numerical results, the papers [10,13,15,17,19,25,31] are followed. The same values of $x \in [0, 100]$, $\mu = 1$, and $x_0 = 40$ and different values of space step h, time step Δt, p, and v are chosen. The experiments are carried out up to $t = 20$.

In the first case, we consider $h = 0.2, 0.1$, $\Delta t = 0.01$, and $v = 0.1, 0.3$. Three invariants and errors are presented in Tables 1 and 2. It is observed from the tables that the changes of three invariants from their initial state are less than 0.03% in all computer runs.

Table 1. Invariants and errors for Example 1 when $x \in [0, 100]$, $h = 0.2$, and $\Delta t = 0.01$.

$\|p=2\|$	I_1		I_2		I_3		$L_2 \times 10^4$		$L_\infty \times 10^4$	
Time	$v=0.1$	$v=0.3$	$v=0.1$	$v=0.3$	$v=0.1$	$v=0.3$	$v=0.1$	$v=0.3$	$v=0.1$	$v=0.3$
0	3.29490	3.58195	0.68342	1.34507	0.02412	0.15372	0.000	0.000	0.000	0.000
5	3.29492	3.58195	0.68342	1.34507	0.02412	0.15372	0.040	0.095	0.029	0.051
10	3.29493	3.58195	0.68342	1.34507	0.02412	0.15372	0.075	0.159	0.035	0.076
15	3.29494	3.58195	0.68342	1.34506	0.02412	0.15372	0.101	0.207	0.036	0.095
20	3.29493	3.58195	0.68342	1.34506	0.02412	0.15372	0.120	0.376	0.066	0.175
$\|p=3\|$	I_1		I_2		I_3		$L_2 \times 10^4$		$L_\infty \times 10^4$	
Time	$v=0.1$	$v=0.3$	$v=0.1$	$v=0.3$	$v=0.1$	$v=0.3$	$v=0.1$	$v=0.3$	$v=0.1$	$v=0.3$
0	4.06256	3.67753	1.13387	1.56573	0.09289	0.22683	0.000	0.000	0.000	0.000
5	4.06258	3.67753	1.13387	1.56573	0.09289	0.22683	0.048	0.217	0.032	0.121
10	4.06260	3.67753	1.13387	1.56573	0.09289	0.22684	0.088	0.400	0.038	0.203
15	4.06261	3.67753	1.13387	1.56573	0.09289	0.22684	0.116	0.581	0.039	0.284
20	4.06260	3.67753	1.13386	1.56572	0.09289	0.22684	0.137	0.918	0.073	0.438
$\|p=4\|$	I_1		I_2		I_3		$L_2 \times 10^4$		$L_\infty \times 10^4$	
Time	$v=0.1$	$v=0.3$	$v=0.1$	$v=0.3$	$v=0.1$	$v=0.3$	$v=0.1$	$v=0.3$	$v=0.1$	$v=0.3$
0	4.55093	3.75921	1.49159	1.72999	0.18389	0.28940	0.000	0.000	0.000	0.000
5	4.55095	3.75921	1.49159	1.72999	0.18389	0.28941	0.059	0.402	0.034	0.231
10	4.55097	3.75921	1.49159	1.72998	0.18389	0.28941	0.106	0.803	0.041	0.421
15	4.55098	3.75921	1.49159	1.72998	0.18389	0.28941	0.142	1.235	0.042	0.627
20	4.55097	3.75921	1.49159	1.72998	0.18389	0.28941	0.176	1.868	0.078	0.915

Table 2. Invariants and errors for Example 1 when $x \in [0, 100]$, $h = 0.1$, and $\Delta t = 0.01$.

$\Vert p = 6 \Vert$	I_1		I_2		I_3		$L_2 \times 10^4$		$L_\infty \times 10^4$	
Time	$v = 0.1$	$v = 0.3$	$v = 0.1$	$v = 0.3$	$v = 0.1$	$v = 0.3$	$v = 0.1$	$v = 0.3$	$v = 0.1$	$v = 0.3$
0	5.12921	3.86622	1.98857	1.94334	0.36740	0.37760	0.000	0.000	0.000	0.000
5	5.12924	3.86622	1.98857	1.94334	0.36740	0.37760	0.236	0.752	0.092	0.402
10	5.12926	3.86622	1.98857	1.94334	0.36740	0.37760	0.458	1.554	0.179	0.823
15	5.12927	3.86622	1.98857	1.94333	0.36740	0.37760	0.661	2.429	0.259	1.282
20	5.12926	3.86622	1.98857	1.94333	0.36740	0.37760	0.848	3.390	0.333	1.785
$\Vert p = 8 \Vert$	I_1		I_2		I_3		$L_2 \times 10^4$		$L_\infty \times 10^4$	
Time	$v = 0.1$	$v = 0.3$	$v = 0.1$	$v = 0.3$	$v = 0.1$	$v = 0.3$	$v = 0.1$	$v = 0.3$	$v = 0.1$	$v = 0.3$
0	5.45779	3.92982	2.30588	2.07217	0.51946	0.43167	0.000	0.000	0.000	0.000
5	5.45781	3.92982	2.30589	2.07217	0.51946	0.43167	0.268	1.204	0.108	0.690
10	5.45783	3.92981	2.30589	2.07216	0.51946	0.43168	0.499	3.012	0.200	1.699
15	5.45785	3.92981	2.30589	2.07214	0.51946	0.43170	0.686	5.690	0.273	3.184
20	5.45784	3.92980	2.30589	2.07212	0.51946	0.43172	0.822	9.520	0.322	5.296
$\Vert p = 10 \Vert$	I_1		I_2		I_3		$L_2 \times 10^4$		$L_\infty \times 10^4$	
Time	$v = 0.1$	$v = 0.3$	$v = 0.1$	$v = 0.3$	$v = 0.1$	$v = 0.3$	$v = 0.1$	$v = 0.3$	$v = 0.1$	$v = 0.3$
0	5.66906	3.97136	2.52266	2.15744	0.63820	0.46614	0.000	0.000	0.000	0.000
5	5.66908	3.97134	2.52266	2.15742	0.63819	0.46615	0.297	2.271	0.124	1.380
10	5.66910	3.97133	2.52266	2.15737	0.63819	0.46620	0.536	7.775	0.220	4.595
15	5.66912	3.97131	2.52267	2.15729	0.63819	0.46629	0.700	19.017	0.280	11.082
20	5.66911	3.97129	2.52267	2.15714	0.63819	0.46643	0.764	39.763	0.288	22.983

Table 3. Errors for Example 1 when $x \in [0, 100]$, $\mu = 1$, and $t = 20$.

			$p = 2$			$p = 3$			$p = 4$		
		$v \rightarrow$	**0.03**	**0.1**	**0.3**	**0.03**	**0.1**	**0.3**	**0.03**	**0.1**	**0.3**
		amp $\rightarrow$	**0.17**	**0.31**	**0.54**	**0.29**	**0.43**	**0.62**	**0.38**	**0.52**	**0.68**
	h	Δt									
$L_2 \times 10^3$	0.1	0.010	1.002	0.044	0.119	1.343	0.062	0.157	1.585	0.073	0.195
	0.2	0.010	0.889	0.012	0.037	1.192	0.013	0.091	1.407	0.017	0.186
	0.1	0.025	1.002	0.064	0.328	1.343	0.109	0.593	1.585	0.158	0.988
	0.2	0.025	0.889	0.025	0.248	1.192	0.055	0.530	1.407	0.101	0.981
	0.1	0.100	1.004	0.488	4.323	1.353	1.035	8.561	1.611	1.795	16.850
	0.2	0.100	0.891	0.452	4.244	1.201	0.986	8.499	1.430	1.741	16.842
$L_\infty \times 10^3$	0.1	0.010	0.403	0.014	0.051	0.541	0.022	0.072	0.638	0.027	0.095
	0.2	0.010	0.403	0.006	0.017	0.541	0.007	0.043	0.638	0.007	0.091
	0.1	0.025	0.403	0.023	0.143	0.541	0.042	0.277	0.638	0.064	0.482
	0.2	0.025	0.403	0.009	0.105	0.541	0.022	0.245	0.638	0.042	0.475
	0.1	0.100	0.403	0.199	1.894	0.541	0.433	4.016	0.638	0.766	8.235
	0.2	0.100	0.403	0.185	1.854	0.541	0.414	3.984	0.638	0.744	8.213

Moreover, it is found that the magnitude of L_2 and L_∞ error norms is adequately small with increasing p, time, and velocity, as expected.

Second, this study seeks to examine the quantity of error norms at different velocities, space steps, and time steps. For this purpose, we have taken $h = 0.1, 0.2$, $\Delta t = 0.01, 0.025, 0.1$, and $v = 0.03, 0.1, 0.3$. The values of L_2 and L_∞ error norms are listed at $t = 20$ in Tables 3 and 4. In these tables, error norms are found to be small enough, and L_∞ error is always

Table 4. Errors for Example 1 when $x \in [0, 100]$, $\mu = 1$, and $t = 20$.

			$p = 6$			$p = 8$			$p = 10$		
		$v \rightarrow$	**0.03**	**0.1**	**0.3**	**0.03**	**0.1**	**0.3**	**0.03**	**0.1**	**0.3**
		amp $\rightarrow$	**0.52**	**0.63**	**0.76**	**0.60**	**0.70**	**0.81**	**0.66**	**0.75**	**0.84**
	h	Δt									
$L_2 \times 10^3$	0.1	0.010	1.900	0.084	0.339	2.094	0.082	0.952	2.225	0.076	3.976
	0.2	0.010	1.686	0.049	0.699	1.858	0.158	2.887	1.974	0.521	13.291
	0.1	0.025	1.901	0.296	2.954	2.095	0.590	12.175	2.228	1.461	57.247
	0.2	0.025	1.686	0.268	3.316	1.859	0.679	14.108	1.976	1.926	66.443
$L_\infty \times 10^3$	0.1	0.010	0.765	0.033	0.178	0.843	0.032	0.529	0.896	0.028	2.298
	0.2	0.010	0.765	0.021	0.366	0.843	0.074	1.591	0.896	0.257	7.601
	0.1	0.025	0.765	0.128	1.563	0.843	0.274	6.802	0.896	0.724	33.005
	0.2	0.025	0.765	0.119	1.750	0.843	0.317	7.808	0.896	0.954	38.021

Table 5. Comparisons of results for Example 1 when $x \in [0, 100]$, and $\mu = 1$.

	Methods	$L_2 \times 10^3$	$L_\infty \times 10^3$	I_1	I_2	I_3
$p = 2$, $v = 1$, $h = 0.2$, $\Delta t = 0.025$, $t = 10$	CBSC-CN [13]	16.3900	9.2400	4.4420	3.2990	1.4130
	CBSC+PA-CN [13]	20.3000	11.2000	4.4400	3.2960	1.4110
	CBSC [17]	9.3019	5.4371	4.4428	3.2998	1.4142
	MFC [19]	3.9140	2.0190	4.4428	3.2997	1.4141
	QBSPG [25]	3.0053	1.6874	4.4428	3.2998	1.4141
	QBSC [15]	2.4155	1.0797	4.4431	3.3003	1.4146
	EBSC [31]	2.3909	1.0647	4.4428	3.2998	1.4142
	Ours-QBSC	2.5893	1.3518	4.4428	3.2997	1.4143
$p = 3$, $v = 0.3$, $h = 0.1$, $\Delta t = 0.01$	QBSPG [25] $t = 5$	0.0409	0.0238	3.6775	1.5657	0.2268
	$t = 10$	0.0719	0.0377	3.6775	1.5657	0.2268
	Ours-QBSC $t = 5$	0.0393	0.0182	3.6776	1.5657	0.2268
	$t = 10$	0.0787	0.0365	3.6776	1.5657	0.2268
$p = 4$, $v = 0.3$, $h = 0.1$, $\Delta t = 0.01$	QBSPG [25] $t = 5$	0.0542	0.0382	3.7592	1.7299	0.2894
	$t = 10$	0.1225	0.0662	3.7592	1.7299	0.2894
	Ours-QBSC $t = 5$	0.0497	0.0244	3.7592	1.7300	0.2894
	$t = 10$	0.0987	0.0483	3.7592	1.7300	0.2894

smaller than L_2 error. Here, it should be noted that if the parameters $h = 0.1$, $\Delta t = 0.01$, and $v = 0.1$ are chosen, then L_∞ error norm remains less than 0.34×10^{-4} during the computer run.

Table 5 reports that the obtained error norms are smaller than those obtained by other methods. In addition, three conservation laws are in agreement with the earlier works.

The behavior of a single solitary wave at different time levels is plotted in Figure 1. Of note, the solitary wave keeps its identity and moves to the right at a constant velocity. By increasing p, a single solitary wave gathers greater energy.

3.2. *Example 2: The collision of two solitary waves*

Consider the governing equation with the following initial condition, which is the linear sum of two well

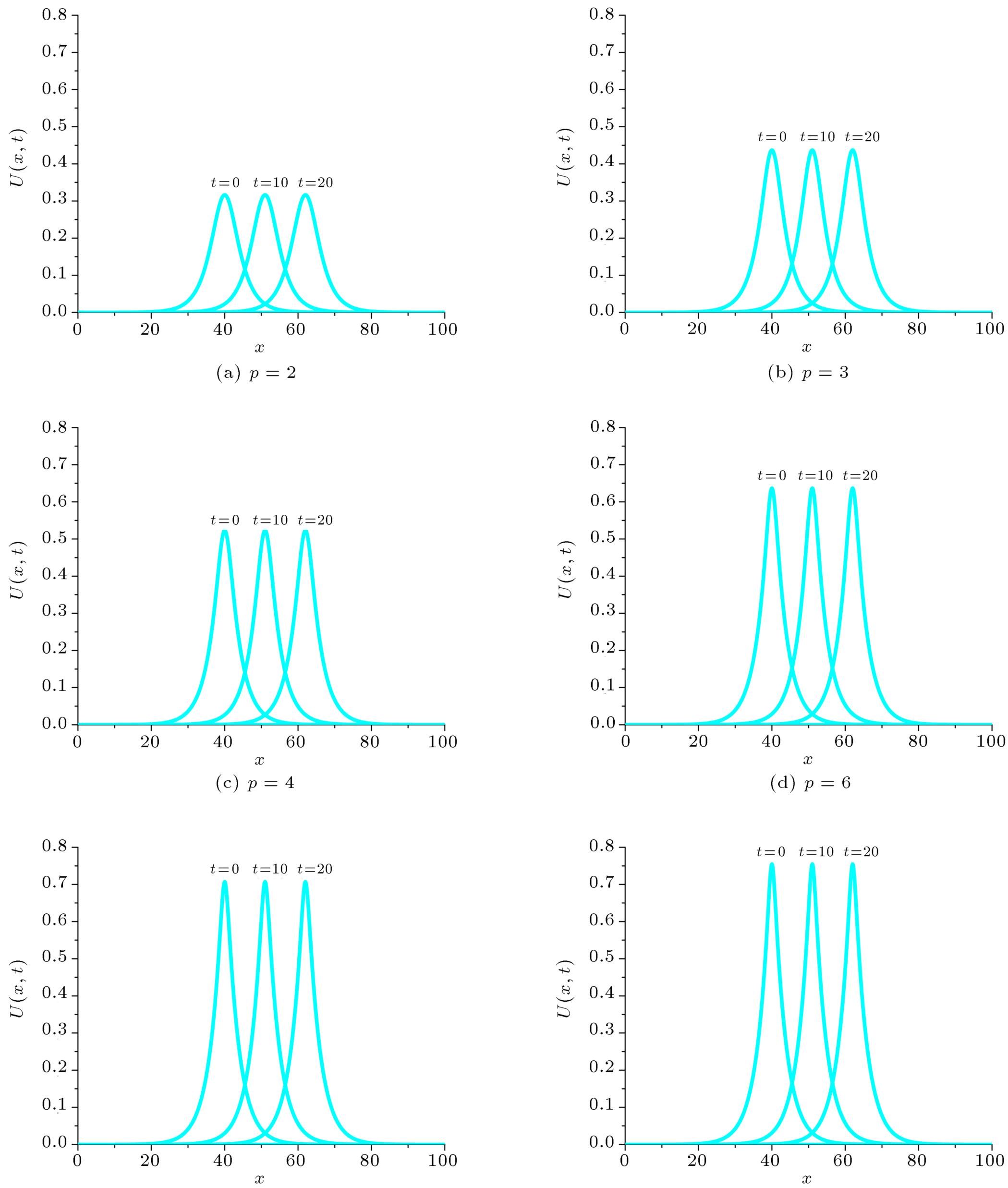

(a) $p = 2$ (b) $p = 3$ (c) $p = 4$ (d) $p = 6$ (e) $p = 8$ (f) $p = 10$

Figure 1. The motion of a single solitary wave when $x \in [0, 100]$, $v = 0.1$, and $x_0 = 40$.

separated solitary waves with different amplitudes

$$U(x,0) = \sum_{i=1}^{2} \sqrt[p]{\frac{v_i(p+2)}{2p}} \sec h^2 \left[\frac{p}{2}\sqrt{\frac{v_i}{\mu(v_i+1)}}(x-x_i) \right], \tag{19}$$

where v_i and x_i, $i = 1, 2$, are arbitrary constants.

Numerical calculation is carried out under the following conditions: $p = 2$, $x \in [0, 250]$, $h = 0.2$, $\Delta t = 0.025$, $\mu = 1$, $v_1 = 4$, $v_2 = 1$, $x_1 = 25$, $x_2 = 55$, $p = 3$, $x \in [0, 120]$, $h = 0.1$, $\Delta t = 0.01$, $\mu = 1$, $v_1 = 48/5$, $v_2 = 6/5$, $x_1 = 20$, $x_2 = 50$, $p = 4$, $x \in [0, 200]$, $h = 0.125$, $\Delta t = 0.01$, $\mu = 1$, $v_1 = 64/3$, $v_2 = 4/3$, $x_1 = 20$, and $x_2 = 80$. The computational data are recorded in Tables 6 and 7, which denote that the quantities of the invariants change a little from their initial count, which are compatible with the results of the referenced paper [25]. The motion of two solitary waves is depicted at different time steps in Figures 2 and 3. As seen in these figures, at time zero, the solitary wave with larger energy is behind the second wave involving smaller energy. According to the solitary wave theory, greater energy means more velocity. Hence, over time, the large wave attains a smaller one and interposition takes place. Similarly, a wave with larger energy leaves behind the second wave with smaller energy, and the same is reiterated.

Table 6. Invariants for Example 2 when $p = 2$, $x \in [0, 250]$, $h = 0.2$, $\Delta t = 0.025$, $\mu = 1$, $v_1 = 4$, $v_2 = 1$, $x_1 = 25$, and $x_2 = 55$.

Time	I_1		I_2		I_3	
	QBSC	**QBSPG**	**QBSC**	**QBSPG**	**QBSC**	**QBSPG**
↓	**Ours**	**[25]**	**Ours**	**[25]**	**Ours**	**[25]**
0	11.4676	11.4677	14.6292	14.6286	22.8803	22.8788
4	11.4676	11.4677	14.6277	14.6292	22.8818	22.8811
8	11.4668	11.4677	14.1399	14.6229	23.3695	22.8798
12	11.4676	11.4677	14.6803	14.6299	22.8292	22.8803
16	11.4676	11.4677	14.6442	14.6295	22.8653	22.8805
20	11.4676	11.4677	14.6309	14.6299	22.8786	22.8806

Table 7. Invariants for Example 2.

Time		**0**	**1**	**2**	**3**	**4**	**5**	**6**
	I_1	9.6907	9.6894	9.6881	9.6851	9.6860	9.6848	9.6835
$p = 3$	I_2	12.9443	12.9433	12.9391	12.3044	12.9704	13.0539	13.0028
	I_3	17.0186	17.0197	17.0239	17.6586	16.9926	16.9091	16.9601
	I_1	8.8342	8.6650	8.5662	8.4965	8.4529	8.4089	8.3702
$p = 4$	I_2	12.1708	11.9332	11.7919	11.6913	11.4644	11.7254	11.5990
	I_3	14.0294	14.2670	14.4083	14.5090	14.7358	14.4748	14.6012

Table 8. Physical quantities for Example 3 when $x \in [-36, 300]$, $x_0 = 0$, $h = 0.1$, $\Delta t = 0.1$, $\mu = 1/6$, $d = 5$, and $U_0 = 0.1$.

Time	I_1			I_2			I_3		
↓	$p = 2$	$p = 3$	$p = 4$	$p = 2$	$p = 3$	$p = 4$	$p = 2$	$p = 3$	$p = 4$
0	3.6049	3.6049	3.6049	0.3372	0.3372	0.3372	0.0014	0.0014	0.0014
50	7.0244	6.9980	6.9954	0.5694	0.5668	0.5665	0.0041	0.0041	0.0041
100	10.3873	10.3343	10.3290	0.7946	0.7893	0.7888	0.0051	0.0051	0.0051
150	13.7503	13.6706	13.6626	1.0198	1.0119	1.0110	0.0061	0.0061	0.0061
200	17.1133	17.0069	16.9961	1.2450	1.2344	1.2333	0.0071	0.0071	0.0071

3.3. Example 3: Undular bore

Finally, we have worked on the growth of an undular bore:

$$U(x,0) = \frac{1}{2}U_0\left[1 - \tanh\left(\frac{x - x_c}{d}\right)\right], \tag{20}$$

which reflects the elevation of the water surface above the equilibrium point. The change in the water level of magnitude Eq. (20) is centered on $x = x_c$. To be consistent with the papers [1,11,12], the parameters $U_0 = 0.1$, $\mu = 1/6$, $h = 0.1$, $\Delta t = 0.1$, $x_c = 0$, $d = 5$, and $x \in [-36, 300]$ are used. The three conservation laws are given in Table 8. From this table, it was observed that the change in the invariants was reasonably small. The undulation profiles at different time steps are drawn in Figures 4 to 6. It can be concluded that the number of undulations increases when the value of x rises and waves move like this for a time. Afterwards, undulations take the peak position and disappear.

4. Conclusion

A collocation method based on quintic B-splines was

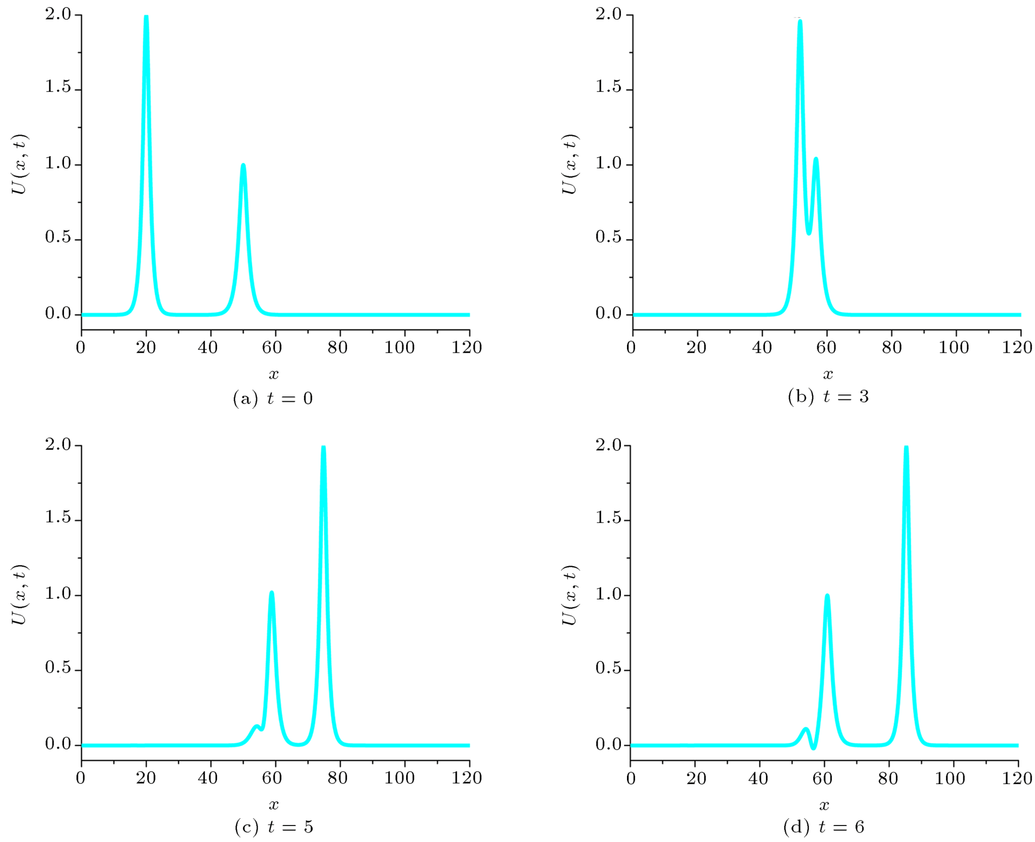

(a) $t = 0$ (b) $t = 3$ (c) $t = 5$ (d) $t = 6$

Figure 2. The collision of two solitary waves at $p = 3$.

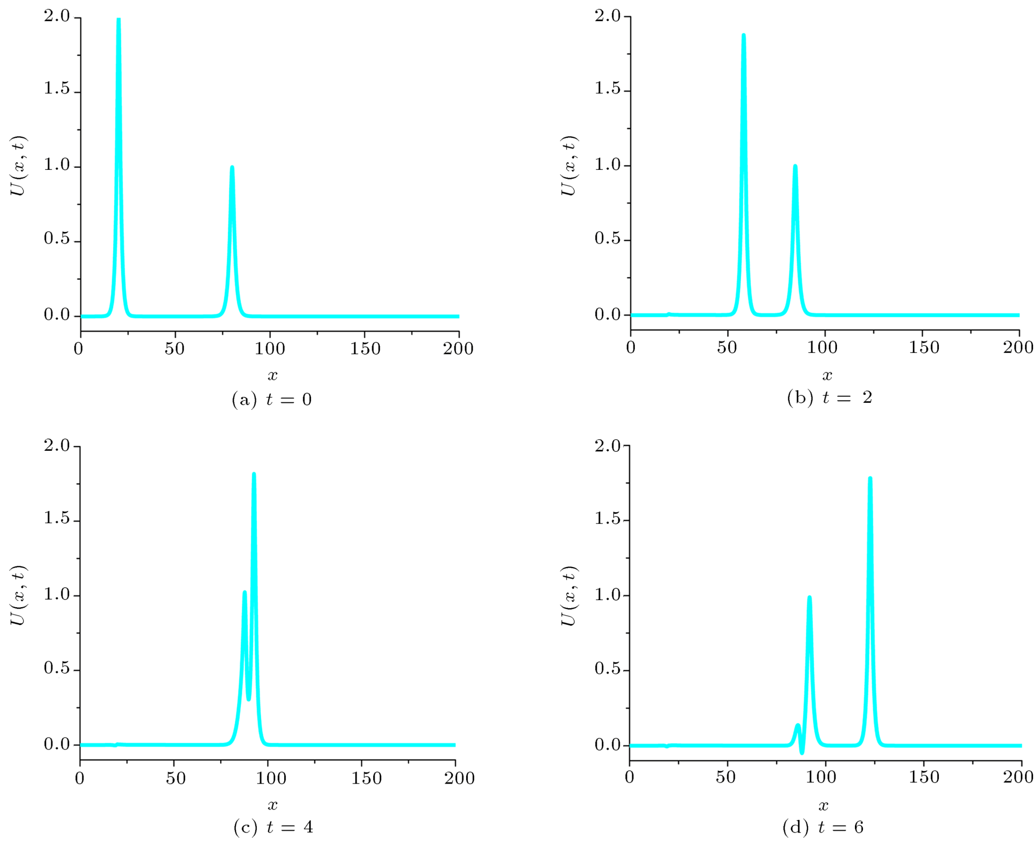

(a) $t = 0$ (b) $t = 2$ (c) $t = 4$ (d) $t = 6$

Figure 3. The collision of two solitary waves at $p = 4$.

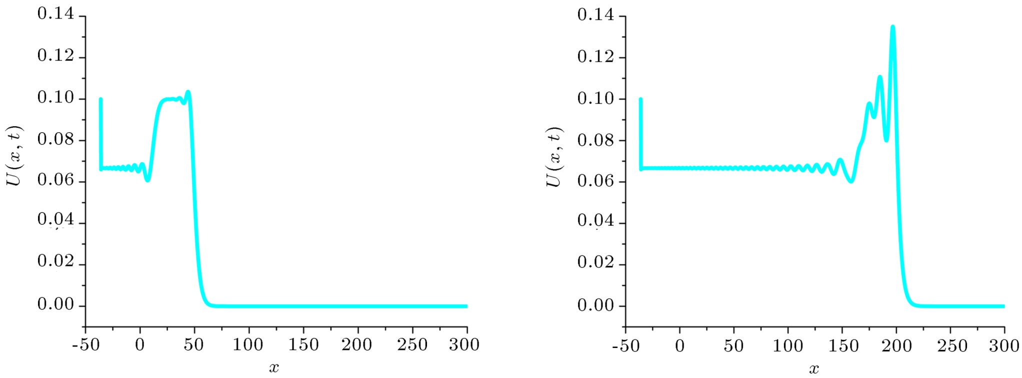

(a) $t = 50$ (b) $t = 200$

Figure 4. The profile of the growth of an undular bore at $p = 2$.

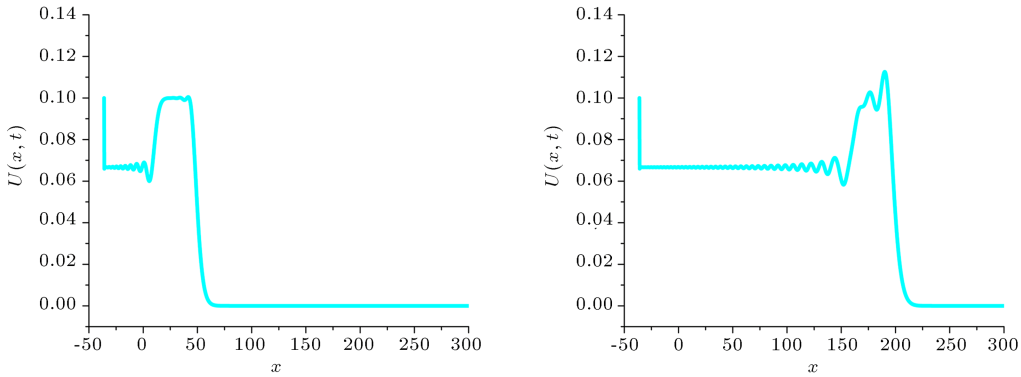

(a) $t = 50$ (b) $t = 200$

Figure 5. The profile of growth of an undular bore at $p = 3$.

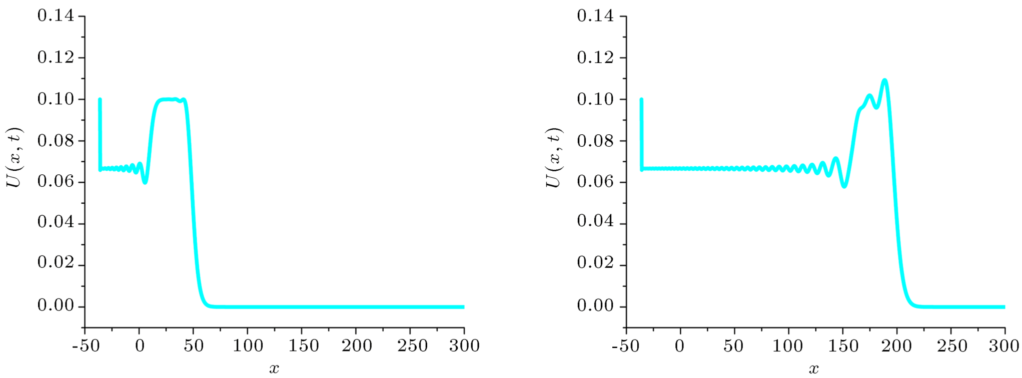

(a) $t = 50$ (b) $t = 200$

Figure 6. The profile of the growth of an undular bore at $p = 4$.

constructed for obtaining a numerical solution to the GRLW equation. Using the von-Neumann technique, the method was shown to be unconditionally stable. The QBSCM was tested with three examples including a single solitary wave, the collision of two solitary waves, and the growth of an undular bore. The error in L_2, and L_∞ norms and three conservative quantities I_1, I_2, and I_3 were calculated to confirm the performance of the numerical scheme. The major point of the QBSCM is that it reduces the problem into a system of first-order ordinary differential equations. Then, the system produces the recurrence relationship whose solutions can be found through the penta-diagonal system. Further to that, it is easy to apply the method to different values of ε and p, which affect the nonlinear term, velocity, and initial condition. The findings prove that three physical quantities of motion remain constant during wave propagation, and the results are the same as those of previous studies. The magnitude of the obtained error norms is adequately small, and it is better than the ones in earlier works. Hereby, the proposed scheme is a practical, accurate and powerful numerical technique. It can be confidingly used for solving similar types of nonlinear problems.

Acknowledgements

The authors are very grateful to anonymous referees for their detailed reading, precious comments, and proposals.

References

1. Peregrine, D.H. "Calculations of the development of an undular bore", *Journal of Fluid Mechanics*, **25**, pp. 321-330 (1966).
2. Peregrine, D.H. "Long waves on a beach", *Journal of Fluid Mechanics*, **27**, pp. 815-827 (1967).
3. Benjamin, T.B., Bona, J.L., and Mahony, J.J. "Model equations for long waves in non-linear dispersive systems", *Philosophical Transactions of the Royal Society of London Series A*, **272**, pp. 47-78 (1972).
4. Morrison, P.J., Meiss, J.D., and Carey, J.R. "Scattering of RLW solitary waves", *Physica D*, **11**, pp. 324-336 (1984).
5. Raslan, K.R. "Collocation method using quadratic B-spline for the RLW equation", *International Journal of Computer Mathematics*, **78**, pp. 399-412 (2001).
6. Dağ, I., Saka, B., and Irk, D. "Application of cubic B-splines for numerical solution of the RLW equation", *Applied Mathematics and Computation*, **159**(2), pp. 373-389 (2004).
7. Saka, B., Dağ, I., and Irk, D. "Quintic B-spline collocation method for numerical solution of the RLW equation", *The ANZIAM Journal*, **49(3)**, pp. 389-410 (2008).
8. Saka, B., Sahin, A., and Dağ, I. "B-spline collocation algorithms for numerical solution of the RLW equation", *Numerical Methods for Partial Differential Equations*, **27**, pp. 581-607 (2011).
9. Soliman, A.A. and Hussien, M.H. "Collocation solution for RLW equation with septic spline", *Applied Mathematics and Computation*, **161**(2), pp. 623-636 (2005).
10. Dağ, I., Saka, B. and Irk, D. "Galerkin method for the numerical solution of the RLW equation using quintic B-splines", *Journal of Computational and Applied Mathematics*, **190**, pp. 532-547 (2006).
11. Esen, A. and Kutluay, S. "Application of a lumped Galerkin method to the regularized long wave equation", *Applied Mathematics and Computation*, **174**, pp. 833-845 (2006).
12. Mei, L. and Chen, Y. "Numerical solutions of RLW equation using Galerkin method with extrapolation techniques", *Computer Physics Communications*, **183**, pp. 1609-1616 (2012).
13. Gardner, L.R.T., Gardner, G.A., Ayoub, F.A., and Amein, N.K. "Approximations of solitary waves of the MRLW equation by B-spline finite element", *Arabian Journal for Science and Engineering*, **22**, pp. 183-193 (1997).
14. Haq, F., Islam, S., and Tirmizi, I.A. "A numerical technique for solution of the MRLW equation using quartic B-splines", *Applied Mathematical Modelling*, **34**(12), pp. 4151-4160 (2010).
15. Karakoç, S.B.G., Yağmurlu, N.M., and Ucar, Y. "Numerical approximation to a solution of the modified regularized long wave equation using quintic B-splines", *Boundary Value Problems*, **2013**, pp. 1-17 (2013).
16. Karakoç, S.B.G., Ak, T., and Zeybek, H. "An efficient approach to numerical study of the MRLW equation with B-spline collocation method", *Abstract and Applied Analysis*, **2014**, pp. 1-15 (2014).
17. Khalifa, A.K., Raslan, K.R., and Alzubaidi, H.M. "A collocation method with cubic B-splines for solving the MRLW equation", *Journal of Computational and Applied Mathematics*, **212**, pp. 406-418 (2008).
18. Raslan, K.R. and EL-Danaf, T.S. "Solitary waves solutions of the MRLW equation using quintic B-splines", *Journal of King Saud University - Science*, **22**(3), pp. 161-166 (2010).
19. Ali, A. "Mesh free collocation method for numerical solution of initial-boundary value problems using radial basis functions", Ph.D. Thesis, Ghulam Ishaq Khan Institute of Engineering Sciences and Technology, Pakistan (2009).
20. Dağ, I., Irk, D., and Sari, M. "The extended cubic B-spline algorithm for a modified regularized long wave equation", *Chinese Physics B*, **22**(4), pp. 1-6 (2013).
21. Abo Essa, Y.M., Abouefarag, I., and Rahmo, E.-D. "The numerical solution of the MRLW equation using the multigrid method", *Applied Mathematics*, **5**, pp. 3328-3334 (2014).
22. Bona, J.L., McKinney, W.R., and Restrepo, J.M. "Stable and unstable solitary-wave solutions of the generalized regularized long-wave equation", *Journal of Nonlinear Science*, **10**, pp. 603-638 (2000).
23. Hammad, D.A. and El-Azab, M.S. "A 2N order compact finite difference method for solving the generalized regularized long wave (GRLW) equation", *Applied Mathematics and Computation*, **253**, pp. 248-261 (2015).
24. Huang, D.M. and Zhang, L.W. "Element-free approximation of generalized regularized long wave equation", *Mathematical Problems in Engineering*, **2014**, pp. 1-10 (2014).
25. Mokhtari, R. and Mohammadi, M. "Numerical solution of GRLW equation using Sinc-collocation method", *Computer Physics Communications*, **181**, pp. 1266-1274 (2010).

26. Roshan, T. "A Petrov-Galerkin method for solving the generalized regularized long wave (GRLW) equation", *Computers and Mathematics with Applications*, **63**, pp. 943-956 (2012).

27. Soliman, A.A. "Numerical simulation of the generalized regularized long wave equation by He's variational iteration method", *Mathematics and Computers in Simulation*, **70**, pp. 119-124 (2005).

28. Zhang, L. "A finite difference scheme for generalized regularized long-wave equation", *Applied Mathematics and Computation*, **168**, pp. 962-972 (2005).

29. Kaya, D. and El-Sayed, S.M. "An application of the decomposition method for the generalized KdV and RLW equations", *Chaos, Solitons and Fractals*, **17**, pp. 869-877 (2003).

30. Hamdi, S., Enright, W.H., Schiesser, W.E., and Gottlieb, J.J. "Exact solutions and invariants of motion for general types of regularized long wave equations", *Mathematics and Computers in Simulation*, **65**, pp. 535-545 (2004).

31. Ramos, J.I. "Solitary wave interactions of the GRLW equation", *Chaos, Solitons & Fractals*, **33**, pp. 479-491 (2007).

32. Mohammadi, R. "Exponential B-spline collocation method for numerical solution of the generalized regularized long wave equation", *Chinese Physics B*, **24**, pp. 1-14 (2015).

33. Zeybek, H. and Karakoç, S.B.G. "A numerical investigation of the GRLW equation using lumped Galerkin approach with cubic B-spline", *SpringerPlus*, **5**, pp. 1-17 (2016).

34. Karakoç, S.B.G. and Zeybek, H. "Solitary-wave solutions of the GRLW equation using septic B-spline collocation method", *Applied Mathematics and Computation*, **289**, pp. 159-171 (2016).

35. Irk, D. and Dağ, I. "Quintic B-spline collocation method for the generalized nonlinear Schrödinger equation", *Journal of the Franklin Institute*, **348**, pp. 378-392 (2011).

36. Ismail, M.S. "Numerical solution of complex modified Korteweg-de Vries equation by collocation method", *Communications in Nonlinear Science and Numerical Simulation*, **14**, pp. 749-759 (2009).

37. Mittal, R.C. and Tripathi, A. "Numerical solutions of generalized Burgers-Fisher and generalized Burgers-Huxley equations using collocation of cubic B-splines", *International Journal of Computer Mathematics*, **93**, pp. 1053-1077 (2015).

38. Ak, T., Karakoç, S.B.G., and Biswas, A. "Application of Petrov-Galerkin finite element method to shallow water waves model: modified Korteweg-de Vries equation", *Scientia Iranica*, **24**, pp. 1148-1159 (2017).

39. Prenter, P.M., *Splines and Variational Methods*, J. Wiley, New York (1975).

40. Rubin, S.G. and Graves, R.A., *A Cubic Spline Approximation for Problems in Fluid Mechanics*, NASA TR R-436, Washington, DC (1975).

Biographies

Halil Zeybek graduated from Ondokuz Mayıs University in 2008 with a BSc degree in Mathematics. He received his MSc and PhD degrees in Applied Mathematics from Nevşehir Hacı Bektaş Veli University in 2011 and 2016, respectively. He is currently a Research Assistant in Abdullah Gul University. He has done his research and publications in the areas of solitary waves, fluid dynamics, numerical analysis, and applied mathematics.

Seydi Battal Gazi Karakoç graduated from Selçuk University in 2001 with a BSc degree in Mathematics. He received his MSc and PhD degrees in Applied Mathematics from İnönü University in 2006 and 2011, respectively. He is currently an Assistant Professor in Nevşehir Hacı Bektaş Veli University. He has done his research and publications in the areas of finite element method, numerical simulation, and applied mathematics.